Organic & Biomolecular Chemistry

Accepted Manuscript

This article can be cited before page numbers have been issued, to do this please use: A. Fumaneri, E. Sisti, A. Ajò, H. S. Varol, V. Bertolotti, L. Menduti and L. De Cola, *Org. Biomol. Chem.*, 2026, DOI: 10.1039/D6OB00479B.

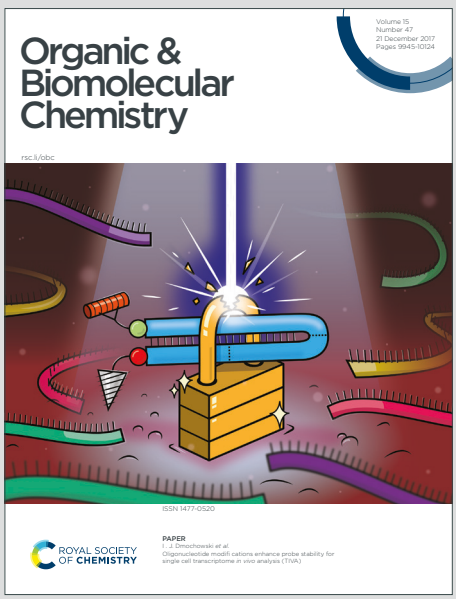

ROYAL SOCIETY OF CHEMISTRY

rsc.li/obc

ARTICLE

View Article Online
DOI: 10.1039/D6OB00479B

Injectable Gelatin-PEG Hydrogels Obtained *via* Cytochrome C-mediated Polymerization

Andrea Fumaneri[+],[1,2] Edoardo Sisti[+],[1,2] Alessandro Ajò,[1,2] H. Samet Varol,[1] Viola Bertolotti,[1] Luigi Menduti,[1*] Luisa De Cola[1,*]

Received 00th January 20xx,
Accepted 00th January 20xx

DOI: 10.1039/x0xx00000x

Injectable hydrogels capable of *in situ* gelation under physiological conditions are highly attractive for minimally invasive surgery and locoregional drug delivery. We herein report three novel injectable hydrogels composed of gelatin methacrylate (**GelMA**) and poly(ethyleneglycol) dimethacrylate (**PEGDA**), crosslinked through a Fenton-like radical polymerization mediated by Cytochrome C (CyC) in the presence of H_2O_2 and L-ascorbic acid. To the best of our knowledge, this is the first example of injectable hydrogel formulation in which CyC is used as redox mediator for the radical polymerization. CyC allows to replace transition-metals while maintaining polymerization kinetics comparable to those obtained for hydrogel synthesized *via* traditional Fenton systems. The resulting hydrogels, undergoing a sol–gel transition within 1.0 and 2.0 minutes, are biocompatible and their properties are highly tunable. Indeed, rheological analysis showed that mechanical properties and the linear viscoelastic region (LVR) can be easily modulated by varying the concentrations of the starting methacryl-functionalized gelatin and crosslinker. Structural characterization and biodegradation studies revealed that enzymatic degradation is strongly dependent on the degree of crosslinking. All hydrogels were readily injectable and showed no detectable cytotoxicity in conditioned media assays. Sustained release of Rhodamine 101, as a drug mimicking system, reached ~70% over 7 days.

Introduction

Hydrogels are three-dimensional (3D) networks composed of cross-linked hydrophilic polymer chains capable of absorbing and retaining large amounts of water or biological fluids.[1]

The chemical and physical properties of hydrogels can be finely tuned through appropriate choice of building blocks/crosslinkers, making these materials versatile and useful for applications in tissue engineering and healing,[2] biosensing/imaging[3] and drug delivery systems.[4] Within these materials, injectable hydrogels have come to the fore as particularly promising platforms for drug delivery applications.[5] They are able to encapsulate therapeutic agents within their three-dimensional network, enabling controlled and sustained release.[6] A major advantage of injectable hydrogels is their minimally invasive administration, as they can be delivered *via* injection without requiring a preformed scaffold.[7] Moreover, being liquids at the injection point, they can fill small spaces and adapt to the shape and volume available. Finally, their intrinsic biocompatibility and porous architecture facilitate oxygen and nutrient diffusion, thereby supporting cell viability.[8] Injectable hydrogels can be classified according to three main criteria: (i) polymer source (natural or synthetic), (ii) structural organization (homo- or copolymeric), and (iii) crosslinking mechanism.

The main crosslinking strategies include ionic interactions[9] and covalent bond formation (radical polymerization,[10] click chemistry,[11] Michael addition,[12] Schiff base formation,[5a] enzymatic crosslinking[13]). Other approaches rely on hydrophobic interactions, host–guest complexation,[14] hydrogen bonding, and stereo-complexation.[15]

Among these, radical polymerization, represents one of the most effective strategies due to its short reaction time, which gives gelation within minutes.[7] A common method to trigger radical polymerization involves the use of light irradiation;[16] however, this approach raises concerns regarding cytotoxicity, site reachability, and patient safety. To address these limitations, redox-initiators can be employed to trigger radical formation.[17]

One of the most widely used approaches to initiate polymerization *via* redox mechanism is the Fenton reaction (FR) capable of generating hydroxyl radicals (·OH) from hydrogen peroxide in the presence of iron ions.[18]

FR has been widely applied to initiate radical polymerization of acrylate- and methacrylate-based polymers and hydrogels[19] and it has found wide applicability in biomedical[20] and environmental applications.[21] Although several hydrogels obtained by conventional FR systems have been described,[22] the use of a biological iron source could be more attractive for in vivo application. We herein report three novel injectable gelatin-based hydrogels obtained *via* radical polymerization triggered by a redox system catalyzed by Cytochrome C (CyC), a low amount of the oxidant H_2O_2 and the water-soluble reducing agent L-ascorbic acid (Fig. 1). Importantly, the use of CyC provides a heme protein-based alternative to free Fe species which, can chelate with proteins/enzymes and alter their biological functions.[23] Control and scavenging experiments supported the role of CyC as a redox mediator, suggesting radical generation associated with the redox activity of the heme center. Hydrogel formation occurs in 1-2 minutes, depending on the formulation. The gelation

[a]*Dipartimento di Scienze Farmaceutiche, Università degli Studi di Milano, via C. Golgi 19, 20133 Milano, Italy.*
Email: luigi.menduti@unimi.it, luisa.decola@unimi.it

[b]*Dipartimento di Biochimica e Farmacologia Molecolare, Istituto di Ricerche Farmacologiche Mario Negri "IRCCS", Via M. Negri 2, Milano, 20156, Italy.*
† These authors contributed equally to this work.

ARTICLE
View Article Online
DOI: 10.1039/D6OB00479B

times are comparable to those of reported injectable hydrogels,[24] or composite hydrogels[25] obtained through conventional Fenton systems, while the storage modulus (G'; 10^3-10^4 Pa) is comparable to that of reported gelatin-based injectable hydrogels.[26]

Beyond rheological properties, the biodegradability, cytocompatibility, and release characteristics of our **Gel-PEG** hydrogels highlight the potential of such materials for locoregional drug delivery over several days.

Results and discussion

Hydrogels synthesis

Injectable **Gel-PEG** hydrogels (Fig. 1A) were obtained *via* radical polymerization initiated by Fenton-like reaction mediated by Cytochrome C (CyC).

To allow for biocompatibility we selected a gelatin (gelatin from porcine skin, type A) as polymeric building block; however pristine gelatin is not reactive in radical polymerization and thus it was functionalized with methacryl groups.

We decided to keep the methacrylation degree low to preserve a fraction of positively charged amino groups which are essential for promoting tissue and cell adhesion; thus gelatin methacrylation was conducted under slight acidic[27] conditions (pH = 5.5, MES buffer; Fig. S1). ^{1}H NMR (Fig. S1) and IR (Fig. S2) analysis confirmed the presence of methacrylate/methacrylamide groups in the **GelMA** polymer.

The total amount of methacryl groups (MA) per mg of gelatin was estimated to be 2.6×10^{-4} $mmol_{MA}/mg_{GelMA}$ (see SI). In line with NMR, Kaiser test conducted pre- and post- functionalization of the gelatin revealed slight variation in the number of amino groups (Fig. S3).

The methacrylated **GelMA** polymer so obtained was therefore employed in the synthesis of injectable **Gel-PEG** hydrogels, using the commercially available **PEGDA** (M_n = 700) as the crosslinker. The radical polymerization of **GelMA** and **PEGDA** was performed by using H_2O_2 as the oxidant and CyC as the iron catalytic source. As reported in the literature,[23] the heme iron center of CyC can react with H_2O_2, leading to the formation of reactive intermediates that may generate hydroxyl radicals. L-ascorbic acid (AA) was employed as sacrificial reducing agent, since ascorbate ($AscH^-$) and ascorbate radical anion ($Asc\cdot^-$) can reduce Fe^{3+}_{CyC} back to Fe^{2+}_{CyC}, restoring the catalytic center while producing a dehydroascorbate (DHA) molecule.[28] Based on literature reports of Fenton systems involving chelated iron species,[23] we proposed a tentative reaction mechanism summarized in eq. 1–4:

1) $Fe^{2+}_{CyC} + H_2O_2 \rightarrow Fe_{Cyc}(H_2O_2)^{2+}$
2) $Fe_{Cyc}(H_2O_2)^{2+} \rightarrow Fe^{3+}_{CyC} + \cdot OH + OH^-$
3) $Fe^{3+}_{CyC} + AscH^- \rightarrow Fe^{2+}_{CyC} + Asc\cdot^- + H^+$
4) $Fe^{3+}_{CyC} + Asc\cdot^- \rightarrow Fe^{2+}_{CyC} + DHA$

To the best of our knowledge, this represents the first example of artificial hydrogel synthesized by Fenton-like radical polymerization using CyC in place of iron salts. With this procedure (see Fig. 1) three injectable hydrogel formulations – **Gel-PEG A** (GelMa 0.47% m/v + PEGDA 8.0% m/v; Fig. 1B), **Gel-PEG B** (GelMa 0.53% m/v + PEGDA 8.9% m/v; Fig. 1B, II), and **Gel-PEG C** (GelMa 0.58% m/v + PEGDA 9.8% m/v; Fig. 1B, III) - were prepared by simultaneously increasing the amount of both gelatin and crosslinker.

The hydrogels exhibited very high and comparable swelling capacities, with swelling ratios (SR%) of 90%, 89%, and 88% for **Gel-PEG A, Gel-PEG B**, and **Gel-PEG C**, respectively.

Extrusion tests demonstrated that all the synthesized materials could be smoothly extruded in PBS from a syringe endowed with an insulin needle, maintaining structural integrity and without needle occlusion (see Movie S1). This property is critical for clinically viable injectable systems and indicates that the polymer ratios in the formulations do not compromise flowability.

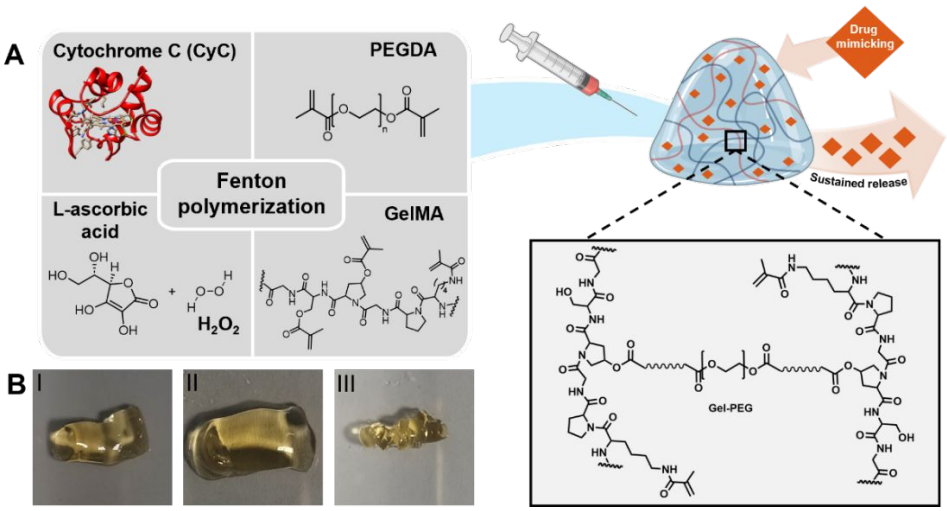

Figure 1. A) Schematic illustration of the preparation of injectable hydrogels *via* Fenton polymerization. Loading and release of a drug mimicking (Rhodamine 101) system. B) Pictures of the three hydrogels obtained: I) **Gel-PEG A**; II) **Gel-PEG B**; III) **Gel-PEG C**.

ARTICLE
View Article Online
DOI: 10.1039/D6OB00479B

The formulation **Gel-PEG B** (Fig. S4) was used as a model system to qualitatively assess the role of CyC in the polymerization mechanism. Control experiments were performed by selectively removing from the reaction mixture: a) the oxidant (H_2O_2), b) the reducing agent (AA) and c) the catalytic source (CyC). Additionally, to assess the involvement of radicals, a scavenging test (d) was performed using 2,2,6,6-Tetramethylpiperidine 1-oxyl (TEMPO).

In detail, when the reaction was performed in the absence of H_2O_2 (a; Fig. S5) or AA (b; Fig. S6), no gelation was observed, which suggested that the radical polymerization is initiated by the H_2O_2/AA system through the generation of reactive radical species, which may include hydroxyl radicals.[29] Accordingly, the control experiment (c) without CyC suggested that the H_2O_2/AA system can generate initiating radical species; however, it results in a slower (> 5 minutes) polymerization process and the formation of a poorly cross-linked gel (Fig. S7). Finally, the scavenging experiment (d) showed that, in the presence of TEMPO, no gelation is observed, consistent with the trapping of propagating radicals and suppression of the radical polymerization (Fig. S8).

The outcomes of the above-described experiments are consistent with a radical-mediated polymerization mechanism, and with the Fenton-like pathway proposed in eq. 1–4. Overall, our results support the role of CyC as a redox mediator contributing to faster polymerization kinetics.

Hydrogels rheological characterization

Gelation kinetics were then evaluated at 37 °C to assess the suitability of the hydrogels for *in-situ* gelation (Fig. 2A). All hydrogels exhibited rapid gelation, with the sol–gel transition defined by the G'–G'' crossover occurring within 2 min (1.7 min for **Gel-PEG A**, 1.5 min for **Gel-PEG B**, and 1.0 min for **Gel-PEG C**). The polymerization reaction reached completion in less than 5 min for all hydrogels, as evidenced by the plateau.

This rapid gelation is advantageous for localized drug delivery, as it minimizes diffusion of liquid precursors and ensures precise spatial confinement of the therapeutic agents. Dynamic mechanical properties were evaluated under both strain test and oscillation frequency model (Fig. 2B, 2C and S9). Increasing the polymer concentration from **Gel-PEG A** to **Gel-PEG C** resulted, as expected, in progressively stiffer hydrogels, as reflected in an increase in the storage modulus (G') (Fig. 2B), compatibly with a denser polymer network and thus enhanced mechanical rigidity.[30] Notably, the rise in stiffness from **Gel-PEG A** to **Gel-PEG B** was accompanied by an expansion of the linear viscoelastic region (LVR), with strain limit (γ) increasing from 13% in **Gel-PEG A** to 33% in **Gel-PEG B** (Fig. S9). This behavior suggests a balance between covalent crosslinking and dynamic non-covalent interactions, generating a network capable of withstanding deformation before structural breakdown. In contrast, further increasing the polymer concentration from **Gel-PEG B** to **Gel-PEG C** resulted in a sharp reduction in LVR (γ = 4%), consistent with a more brittle structure (Fig. S9).

These findings indicate that increasing polymer content enhances stiffness (higher G') but reduces the strain range over which the hydrogels behave linearly, consistent with a lower critical strain. Oscillatory frequency sweeps performed at a fixed strain amplitude within the LVR (Fig. S9) showed predominantly elastic behavior (G'>G'') at low frequencies, with a G'-G'' crossover occurring at 9-10 Hz for all hydrogels. Moreover, a step–strain recovery test was performed to evaluate the self-healing properties of the formulated hydrogels (Fig. 2C).

The results showed that **Gel-PEG A** only partially recovers its stiffness, and this trend remains consistent across all creep–recovery cycles. This behavior is likely attributable to the breaking of covalent bonds within the hydrogel network, which limits the complete reformation of the three-dimensional structure. Conversely, **Gel-PEG B** and **Gel-PEG C** exhibited full recovery of both G' and G" values after each creep phase, suggesting that the applied deformation did not significantly affect the crosslinking network. Interestingly, the order of mixing the components is critical for obtaining gels with the described properties. In fact, the syringe must be loaded with the solution containing GelMA, the PEGDA crosslinker, and CyC first, and then with the solution containing the oxidant and ascorbic acid (AA).

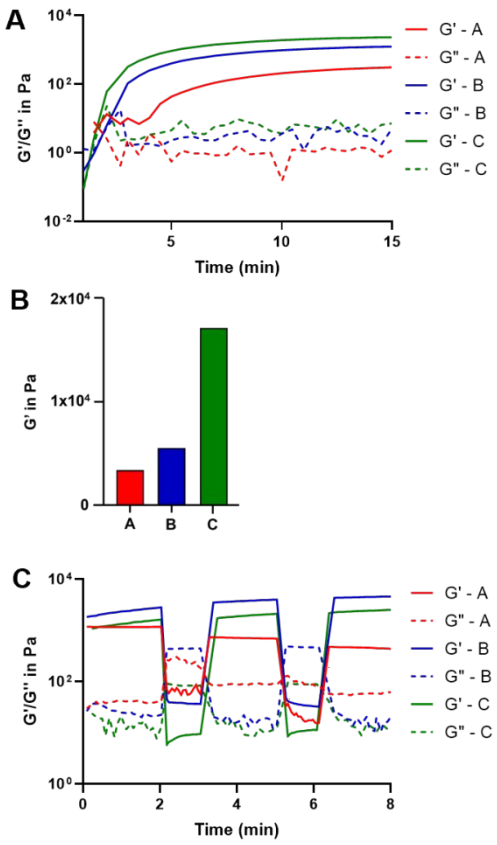

Figure 2. A) gelation kinetics of: **Gel-PEG A-C**; B) elastic modulus of **Gel-PEG A-C**, (data is represented as mean); C) Step-strain recovery test of **Gel-PEG A-C** at a strain of γ%=1 (t = 2 min) and at a strain of 500% (t = 1 min).

ARTICLE
View Article Online
DOI: 10.1039/D6OB00479B

Hydrogels structural characterization

The microscopic structure of the hydrogels was assessed by Scanning Electron Microscopy (SEM) analysis of freeze-dried samples (Fig. 3A; see Supplementary Methods). It should be noted that the observed pore morphology corresponds to the lyophilized hydrogel state and may differ from the native hydrated structure due to structural rearrangements induced during freeze-drying. Nevertheless, since all hydrogel formulations were subjected to the same lyophilization protocol, SEM analysis still enables comparative evaluation of differences in pore density, pore size uniformity, and overall network organization between the samples.

The SEM images show that all hydrogels possess a porous three-dimensional microstructure with interconnected pores, while also displaying differences in pore density, pore size uniformity, and overall network organization depending on the formulation. Compared to **Gel-PEG A** and **Gel-PEG B**, **Gel-PEG C** exhibits a lower pore density and a more compact microarchitecture (Fig. 3A-III). This could explain the more brittle structure of **Gel-PEG C**, as the denser network may limit chain mobility and reduce the network's ability to dissipate mechanical energy under load.[31] The degradation profile of **Gel–PEG** hydrogels after incubation in Collagenase A showed a gradual decrease in mass loss with increasing polymer concentration, ultimately resulting in no detectable degradation for **Gel-PEG C** (Fig. 3B). This trend can be attributed to the higher density of chemical crosslinks, which reduces the susceptibility of GelMA to enzymatic hydrolysis. To confirm the successful incorporation of PEGDA into the hydrogel matrix, ATR-IR (Attenuated Total Reflection Infrared Spectroscopy) spectra of lyophilized samples were recorded (Fig. 3C). The C–O stretching vibration (1080 cm^{-1}) showed increased intensity compared to pristine **GelMA**, consistent with the ether bonds of the PEGDA crosslinker. Moreover, the spectra exhibited a stronger C–H sp^3 stretching band at 2880 cm^{-1}, again attributable to the PEGDA chains. A decrease in the C=C stretching band, typical of GelMa,[32] at 1640 cm^{-1} was also observed, according with the conversion of methacrylic double bonds in the radical polymerization.

Thermogravimetric analysis (TGA) confirmed that **Gel-PEG A-C** undergo complete thermal degradation (Fig. S11). A first mass loss at 162–169 °C was attributed to the release of water strongly bound to the gelatin through polar interactions, as previously reported for gelatin materials.[33] The second degradation event, occurring at 270–290 °C, corresponded to **GelMA** decomposition. A third step at 376–380 °C was assigned to degradation of the PEGDA units, followed by a final event at 440–450 °C associated with the residual **GelMA** fraction, leading to the full thermal decomposition of the network.

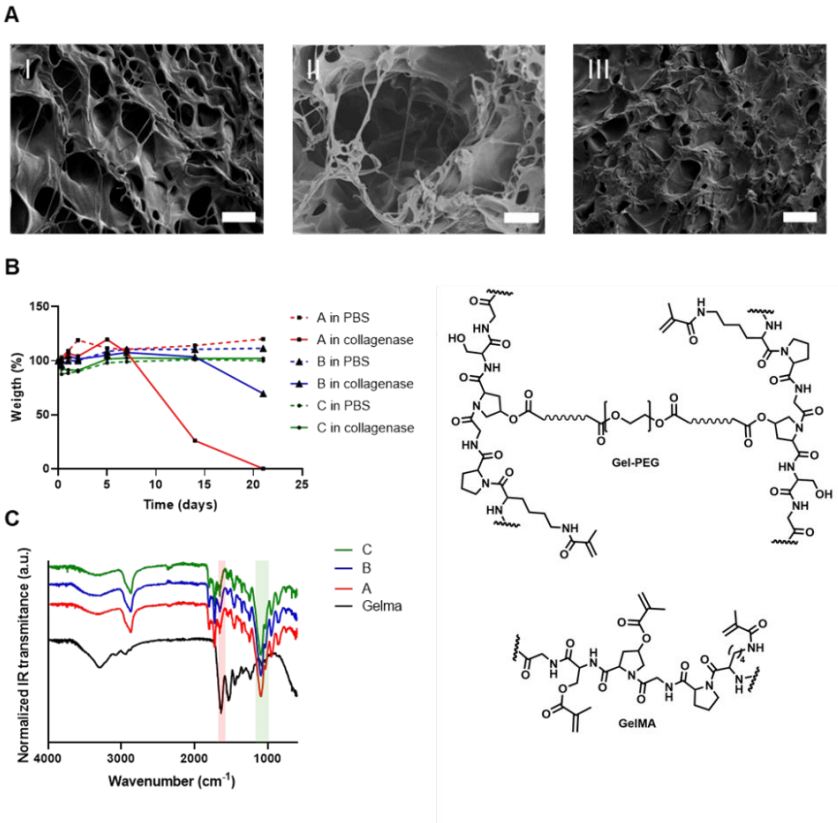

Figure 3. A) SEM images of I) **Gel-PEG A**, II) **Gel-PEG B**, and III) **Gel-PEG C** - scale bar is 50 µm; B) degradation kinetics of **Gel-PEG A-C** in Collagenase A (1 mg/mL in PBS, solid lines) and PBS (dashed lines); C) ATR-IR spectra of GelMa and Hydrogel A, B and C - spectra normalized by the intensity of the of C-O frequency (2880 cm^{-1}).

ARTICLE
View Article Online
DOI: 10.1039/D6OB00479B

Hydrogels biocompatibility and release profile

Cell culture assays were carried out to evaluate the biosafety of compounds released from the gels after gelation. Since the proposed hydrogels have been developed within the context of locoregional therapeutic strategies for hepatic applications, Human Hepatoma G2 (HepG2) cells were selected as model cell line for preliminary biological assessment. In detail, HepG2 cells were treated with **Gel-PEG A**, **B** and **C** and cell viability tests were performed after 24 and 48 h (Fig. 4A and 4B) using MTT assay (λ_{abs} = 565 nm; see SI). After 24 and 48 h (Fig 4A, 4B), no differences were observed in the cell viability by comparing untreated cells (labelled as **Untr**) and cells treated with the hydrogels (labelled as **Gel-PEG A**, **B** and **C**); this suggested that none of the hydrogels releases cytotoxic by-products. We next sought to perform sustained release studies on **Gel-PEG B**, which revealed to be the formulation combining the best properties in terms of rapid gelation, preserved injectability, and extended linear viscoelastic region.

A release assay was performed using **Gel-PEG B** and, the water-soluble dye Rhodamine 101[34] (Fig. 4C) as drug-mimicking. The dye was loaded in the hydrogel B at a concentration of 0.13 mg/mL and then incubated (37°C in a humidified atmosphere) in PBS. Cumulative release was determined by measuring the emission intensity (λ_{em} = 595 nm) of the supernatant at each timepoint (see SI). After the initial burst that reaches the 50% within 24h, the release profile gradually approached a plateau, reaching about 70% cumulative release after 7 days. After 15 days more than 90% of the dye was released by the hydrogel. The observed burst release (≈ 50% in 24 h) may be attributed to the heterogeneous distribution of rhodamine 101 within the hydrogel network. In detail, the dye molecules located close the surface diffuse rapidly into the surrounding medium; conversely, the dye molecules located in the core of the hydrogel network display limited diffusion, resulting in a slower release.

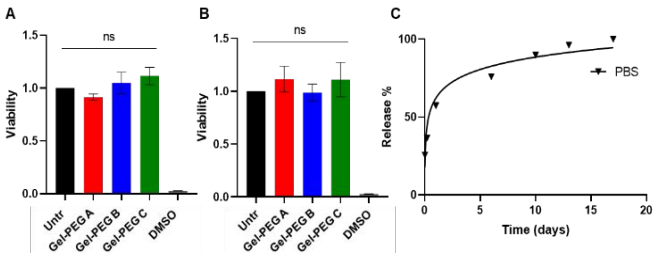

Figure 4. Cell viability test at A) 24 h and B) 48 h of incubation; results are expressed as mean ±SD (N = 3) - one-way ANOVA statistics analysis with Šídák's post hoc multiple comparisons test was used (ns: $p > 0.05$); C) Release of free Rhodamine 101 embedded in hydrogel in PBS at 37°C (data is represented as mean).

Conclusions

Three fast gelating (1-2 minutes) and biodegradable, injectable **Gel-PEG** hydrogels (**Gel-PEG A-C**) were synthesized *via* Fenton-like radical polymerization reactions mediated by Cytochrome C (CyC). We have demonstrated that it is possible to modulate the gelation time, stiffness, and degradation kinetics by simply varying the concentrations of **GelMA** and **PEGDA**. Our combined structural, rheological and release studies showed that **Gel-PEG B** is the most promising formulation in that it combines rapid gelation (1.5 min) and preserved injectability, conserved linear viscoelastic region (LVR) and mechanical strength along with biodegradability and good cargo-release performances (70% release over 7 days).

Overall, the hydrogels presented in this work represent a promising platform for the construction of fast-injectable formulations allowing for localized drug-release.

Author contributions

AF: synthesis of the hydrogels, characterization and biological tests; ES: synthesis of the hydrogels, characterization and biological tests; AA: synthesis of the hydrogels; HSV: SEM experiments, data analysis; VB: synthesis of the hydrogels; LM: mechanistic experiments, supervision and conceptualization, data analysis, writing&review; LDC: conception of the idea, supervision and conceptualization, writing&review, funding acquisition. All the authors discussed and commented on the manuscript.

Conflicts of interest

The authors declare no conflict of interest.

Data availability

The data supporting this article have been included as part of the Supplementary Information.

Acknowledgements

We gratefully acknowledge Project Next Gen EU and MUR as PNRR M4C2, "Mano-HCC", PE_00000019, HEAL ITALIA, CUP E93C22001860006. H.S.V. sincerely thanks the Alexander von Humboldt Foundation for financial support.

References

1 a) H. Zeng, Y. Han, H. Li, X. Niu, L. Chen, D. Zhang and K. Wang, *J. Mater. Chem. C*, 2025, **13**, 14101; b) S. Bashir, M. Hina, J. Iqbal, A. H. Rajpar, M. A. Mujtaba, N. A. Alghamdi, S. Wageh, K. Ramesh and S. Ramesh, *Polymers*, 2020, **12**, 2702; c) T.-C. Ho, C.-C. Chang, H.-P. Chan, T.-W. Chung, C.-W. Shu, K.-P. Chuang, T.-H. Duh, M.-H. Yang and Y.-C. Tyan, *Molecules*, 2022, **27**, 2902.

2 a) S. Mantha, S. Pillai, P. Khayambashi, A. Upadhyay, Y. Zhang, O. Tao, H. M. Pham and S. D. Tran, *Materials*, 2019, **12**, 3323; b) P.

ARTICLE
View Article Online
DOI: 10.1039/D6OB00479B

Bertsch, M. Diba, D. J. Mooney and S. C. Leeuwenburgh, *Chemical Reviews*, 2022, **123**, 834–873.

3 a) M. A. Mohamed, A. Fallahi, A. M. El-Sokkary, S. Salehi, M. A. Akl, A. Jafari, A. Tamayol, H. Fenniri, A. Khademhosseini and S. T. Andreadis, *Progress in polymer science*, 2019, **98**, 101147; b) A. Herrmann, R. Haag and U. Schedler, *Advanced Healthcare Materials*, 2021, **10**, 2100062; c) D.-M. Radulescu, I. A. Neacsu, A.-M. Grumezescu and E. Andronescu, *Polymers*, 2022, **14**, 799; d) F. Fiorini, E. Longhi, A. Lazaro, D. Di Prisco, G. Tamboia, G. Alonci, L. Menduti and L. De Cola, *Chemistry–A European Journal*, 2025, **31**, e202404572.

4 a) H. Van der Linden, S. Herber, W. Olthuis and P. Bergveld, *Analyst*, 2003, **128**, 325–331; b) M. Hamidi, A. Azadi and P. Rafiei, *Advanced Drug Delivery Reviews*, 2008, **60**, 1638–1649; c) A. Singh, P. K. Sharma, V. K. Garg and G. Garg, *Int. J. Pharm. Sci. Rev. Res*, 2010, **4**, 97–105; d) L. Zhang, K. Li, W. Xiao, L. Zheng, Y. Xiao, H. Fan and X. Zhang, *Carbohydrate Polymers*, 2011, **84**, 118–125; e) E. M. Ahmed, *Journal of Advanced Research*, 2015, **6**, 105–121; f) Y. Cheng, H. Zhang, H. Wei and C.-Y. Yu, *Biomaterials Science*, 2024, **12**, 1151–1170; g) M. Jyothika, S. J. Gowda, G. K. Kumar, K. Rakshitha, K. Srikruthi, P. Goudanavar and N. R. Naveen, *Biomedical Materials & Devices*, 2026, **4**, 62–77.

5 a) Q. V. Nguyen, D. P. Huynh, J. H. Park and D. S. Lee, *European Polymer Journal*, 2015, **72**, 602–619; b) G. Alonci, F. Fiorini, P. Riva, F. Monroy, I. López-Montero, S. Perretta and L. De Cola, *ACS Applied Bio Materials*, 2018, **1**, 1301–1310; c) M. E. Giménez, C. F. Davrieux, E. Serra, M. Palermo, E. J. Houghton, G. Alonci, E. Piantanida, A. Garcia Vazquez, V. Lindner and B. Dallemagne, *Hernia*, 2019, **23**, 1175–1185; d) E. Piantanida, G. Alonci, A. Bertucci and L. De Cola, *Accounts of chemical research*, 2019, **52**, 2101–2112; e) E. Piantanida, I. Boškoski, G. Quero, C. Gallo, Y. Zhang, C. Fiorillo, V. Arena, G. Costamagna, S. Perretta and L. De Cola, *Materials Today Bio*, 2021, **10**, 100109; f) J. M. Zuidema, A. Ajò, M. Carofiglio and L. De Cola, *ACS omega*, 2025, **11**, 746–756.

6 a) W. Shen, X. Chen, J. Luan, D. Wang, L. Yu and J. Ding, *ACS Applied Materials & Interfaces*, 2017, **9**, 40031–40046; b) C. Hu, F. Zhang, L. Long, Q. Kong, R. Luo and Y. Wang, *Journal of controlled release : official journal of the Controlled Release Society and the Japanese Society of drug delivery system*, 2020, **324**, 204–217; c) G. Dalei, S. Das, S. R. Jena, D. Jena, J. Nayak and L. Samanta, *Chemical Engineering Science*, 2023, **269**, 118482; d) W. Zhu, Y. Zhao, Z. Wu, F. Lv, Y. Zhang and S. Guo, *Polymer*, 2023, **264**, 125535.

7 S. Almawash, S. K. Osman, G. Mustafa and M. A. El Hamd, *Pharmaceuticals*, 2022, **15**, 371.

8 J. I. Paez and K. S. Lim, *J. Mater. Chem. B*, 2024, **12**, 5571–5572.

9 E. Y. Du, H. T. K. Duong, M. A. K. Tolentino, J. L. Houng, P. Suwannakot, K. C. Tjandra, D. H. T. Nguyen, R. D. Tilley and J. Justin Gooding, *Macromolecular Research*, 2025, **33**, 921–931.

10 a) P. M. Chichiricco, R. Riva, J.-M. Thomassin, J. Lesoeur, X. Struillou, C. Le Visage, C. Jérôme and P. Weiss, *Dental Materials*, 2018, **34**, 1769–1782; b) S. L. Fenn and R. Floreani, *Journal of Biomedical Materials Research Part B: Applied Biomaterials*, 2016, **104**, 1229–1236; c) T.-U. Nguyen, K. E. Watkins and V. Kishore, *Journal of Biomedical Materials Research Part A*, 2019, **107**, 1541–1550.

11 V. Crescenzi, L. Cornelio, C. Di Meo, S. Nardecchia and R. Lamanna, *Biomacromolecules*, 2007, **8**, 1844–1850.

12 a) R. F. N. Quadrado, K. L. Macagnan, A. S. Moreira and A. R. Fajardo, *International Journal of Biological Macromolecules*, 2021, **193**, 1032–1042; b) O. Guaresti, S. Basasoro, K. González, A. Eceiza and N. Gabilondo, *European Polymer Journal*, 2019, **119**, 376–384.

13 R. Jin, L. S. Moreira Teixeira, P. J. Dijkstra, C. A. van Blitterswijk, M. Karperien and J. Feijen, *Biomaterials*, 2010, **31**, 3103–3113.

14 Q. Feng, K. Wei, S. Lin, Z. Xu, Y. Sun, P. Shi, G. Li and L. Bian, *Biomaterials*, 2016, **101**, 217–228.

15 S. R. Van Tomme, A. Mens, C. F. van Nostrum and W. E. Hennink, *Biomacromolecules*, 2008, **9**, 158–165.

16 M. Chen, M. Zhong and J. A. Johnson, *Chemical reviews*, 2016, **116**, 10167–10211.

17 A. S. Sarac, *Progress in Polymer Science*, 1999, **24**, 1149–1204.

18 a) D. Meyerstein, *Nature Reviews Chemistry*, 2021, **5**, 595–597; b) J. Xiao, S. Guo, D. Wang and Q. An, *Chemistry–A European Journal*, 2024, **30**, e202304337.

19 A. Reyhani, T. G. McKenzie, Q. Fu and G. G. Qiao, *Macromolecular Rapid Communications*, 2019, **40**, 1900220.

20 Z. Tang, P. Zhao, H. Wang, Y. Liu and W. Bu, *Chemical reviews*, 2021, **121**, 1981–2019.

21 N. Wang, T. Zheng, G. Zhang and P. Wang, *Journal of Environmental Chemical Engineering*, 2016, **4**, 762–787.

22 a) J. A. G. Barros, G. J. M. Fechine, M. R. Alcantara and L. H. Catalani, *Polymer*, 2006, **47**, 8414–8419; b) L. Sun, S. Zhang, J. Zhang, N. Wang, W. Liu and W. Wang, *Journal of Materials Chemistry B*, 2013, **1**, 3932–3939; c) J. Y. Kim, S. B. Ryu and K. D. Park, *Journal of industrial and engineering chemistry*, 2018, **58**, 105–112; d) J. Choi, M. McGill, N. R. Raia, O. Hasturk and D. L. Kaplan, *Advanced Healthcare Materials*, 2019, **8**, 1900644; e) J. Choi, O. Hasturk, X. Mu, J. K. Sahoo and D. L. Kaplan, *Biomacromolecules*, 2021, **22**, 773–787.

23 C.C. Winterbourn, *Toxicology Letters*, 1995, **82/83**, 969-974.

24 a) L. Sun, S. Zhang, J. Zhang, N. Wang, W. Liu, W. Wang, *Journal of Material Chemistry B*, 2013, **1**, 3932-3939; b) J. Choi, M. McGill, N. R. Raia, O. Hasturk, D.L. Kaplan, *Advanced Healthcare Materials* 2019, **8**, 1900644; c) J. Choi, O. Hasturk, X. Mu, J. K. Sahoo and D. L. Kaplan, *Biomacromolecules*, 2021, **22**, 773–787.

25 a) D.H. Oh, P.L. Thi, K.D. Park, *ACS Applied Bio Materials*, 2024, **7**, 5702−5718; b) L. Wang, H. Guo, W. Zhang, X. Li, Z. Su, X. Huang, *Materials Today Bio*, 2024, **29**, 101297.

26 a) S.T. Koshy, R.M. Desai, P. Joly, J. Li, R.K. Bagrodia, S.A. Lewin, N.S. Joshi, D.J. Mooney, *Advanced Healthcare Materials*, 2016, **5**, 541–547; b) Z. Li, T. Qu, C. Ding, C. Ma, H. Sun, S. Li, X. Liu, *Acta Biomaterialia*, 2015, **13**, 88–100; c) Y. Dong, Sigen A, M. Rodrigues, X. Li, S.H. Kwon, N. Kosaric, S. Khong, Y. Gao, W. Wang, G.C. Gurtner, *Advanced Functional Materials*, 2017, **27**, 1606619.

27 K. Valente, G. N. Boice, C. Polglase, R. G. Belli, E. Bourque, A. Suleman and A. Brolo, *Pharmaceutics*, 2024, **16**, 1016.

ARTICLE

View Article Online
DOI: 10.1039/D6OB00479B

28 J. Bolobajev, M. Trapido, A. Goi, *Chemical Engineering Journal*, 2015, **281**, 566–574.

29 M .Chausson. A.-S. Fluchère, E. Landreau, Y. Aguni, Y. Chevalier, T. Hamaide, N. Abdul-Malak, I. Bonnet, *International Journal of Pharmaceutics*, 2008, **362**, 153-162.

30 a) L. Hsu, C. Weder and S. J. Rowan, *Journal of Materials Chemistry*, 2011, **21**, 2812–2822; b) J. Karvinen, T. O. Ihalainen, M. T. Calejo, I. Jönkkäri and M. Kellomäki, *Materials Science and Engineering: C*, 2019, **94**, 1056–1066; c) H. S. Varol, A. Srivastava, S. Kumar, M. Bonn, F. Meng and S. H. Parekh, *Polymer*, 2020, **200**, 122529.

31 E. C. Lloyd, S. Dhakal, S. Amini, R. Alhasan, P. Fratzl, D. R. Tree, S. Morozova and R. J. Hickey, *Nature Communications*, 2025, **16**, 3792.

32 R. Rajalekshmi, S. Unnikrishnan, L. Krishnan and K. Krishnan, *Journal of Applied Polymer Science*, DOI:10.1002/app.44529.

33 B. Velasco-Rodriguez, T. Diaz-Vidal, L. C. Rosales-Rivera, C. A. García-González, C. Alvarez-Lorenzo, A. Al-Modlej, V. Domínguez-Arca, G. Prieto, S. Barbosa, J. F. A. Soltero Martínez, P. Taboada, *International Journal of Molecular Sciences.*, 2021, **22**, 6758.

34 H. S. Varol, D. Kaya, E. Contini, C. Gualandi and D. Genovese, *Materials Advances*, 2024, **5**, 8351–8383.

View Article Online
DOI: 10.1039/D6OB00479B

Data availability

The data supporting this article have been included as part of the Supplementary Information.